Time-reversal imaging of seismic sources and application to the great Sumatra earthquake

Carene Larmat,[1,2] Jean-Paul Montagner,[1] Mathias Fink,[3] Yann Capdeville,[1] Arnaud Tourin,[3] and Eric Clévédé[1]

[1] The increasing power of computers and numerical methods (like spectral element methods) allows continuously improving modelization of the propagation of seismic waves in heterogeneous media and the development of new applications in particular time reversal in the three-dimensional Earth. The concept of time-reversal (hereafter referred to as TR) was previously successfully applied for acoustic waves in many fields like medical imaging, underwater acoustics and non destructive testing. We present here the first application at the global scale of TR with associated reverse movies of seismic waves propagation by sending back long period time-reversed seismograms. We show that seismic wave energy is refocused at the right location and the right time of the earthquake. When TR is applied to the Sumatra-Andaman earthquake (26 Dec. 2004), the migration of the rupture from the south towards the north is retrieved. Therefore, TR is potentially interesting for constraining the spatio-temporal history of complex earthquakes. **Citation:** Larmat, C., J.-P. Montagner, M. Fink, Y. Capdeville, A. Tourin, and E. Clévédé (2006), Time-reversal imaging of seismic sources and application to the great Sumatra earthquake, *Geophys. Res. Lett.*, *33*, L19312, doi:10.1029/ 2006GL026336.

1. Introduction

[2] The occurrence of the disastrous Sumatra-Andaman earthquake on Dec. 26, 2004 makes it necessary to develop innovative techniques for studying the complex spatio-temporal characteristics of rupture. In this paper, we propose to use a Time Reversal technique. TR is based on both the source-receiver reciprocity and the time invariance of the wave equation in non dissipative media, which only contains a second-order derivative. Thus, for every burst of sound diverging from a source-and possibly reflected, refracted or scattered- the set of waves that precisely retraces all of the complex paths and that converges in synchrony at the original source (as if time were going backwards) is also solution. The existence of acoustic transducers which can be used as both receivers and emitters made possible the implementation of time-reversal experiments in laboratory (Figure 1). First, a transducer array records the field radiated by an acoustic source. Then

the records are time-reversed and retransmitted through the medium by the same array acting as a time-reversal mirror (TRM). The resulting wave travels back and refocuses at the initial source position. The numerous performed TRM experiments by *Fink* [1996, 1997] and *Fink et al.* [2003] have shown that the TR technique is robust in a great variety of configurations and that a high degree of heterogeneity in the propagation medium ensures a large virtual aperture of the receiver set because the information in time compensates the lack of information in space. TR thus appears as a good technique for target detection in complex media or reverberant cavities, which leads to numerous applications in medical imaging, communication or non destructive testing. It must be pointed out that despite disorder, small errors inevitably introduced during the recording and re-emitting phases do not perturb significantly the refocusing [*Tourin et al.*, 2001].

[3] In seismology, the elasto-dynamic equation that describes elastic waves in isotropic solid is more complex but both time-reversal invariance and spatial reciprocity are still valid.

2. Application of Time-Reversal Method to Seismic Sources

[4] First attempts of TR with seismic waves was made by *Rietbrock and Scherbaum* [1994] at local scale with the acoustic equation. A good focusing is expected to be easier at the global scale than at the regional scale, as the Earth is a spherical cavity, including reflecting boundaries. In comparison with acoustics, we are facing specific issues in the seismological case. Firstly, seismic waves are 3-component elastic waves. Secondly, it is of course impossible to propagate the time-reversed waves in the Earth as in the forward propagation medium. In contrast to pure ''experimental'' applications in acoustics, the real Earth, the medium where the wave field is generated and propagates, and the virtual medium where the time reversal experiment (necessarily numerical) is performed, are different. In this paper, we used 2 different numerical methods, the normal mode summation technique [*Gilbert and Dziewonski*, 1975] and the method coupling the spectral element method and the modal solution [*Capdeville et al.*, 2003]. The first method is very accurate for 1D models such as PREM whereas the second method works well for general heterogeneous 3D-models. The coupled method combines the speed and the low cost of normal mode summation and the geometrical flexibility of the spectral element method (however it is more expensive and time-consuming). The use of a virtual Earth model to backpropagate the time-reversed field makes the choice of the duration of the time-

---
[1]Equipe de Sismologie, Institut de Physique du Globe de Paris, Paris, France.
[2]Now at Seismological Laboratory, California Institute of Technology, Pasadena, California, USA.
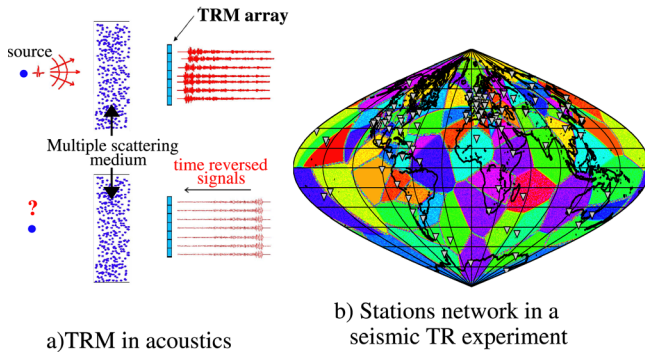[3]Laboratoire Ondes et Acoustique, ESPCI, Paris, France.

Figure 1. (a) Principle of Time Reversal Method applied to a multiple scattering medium. (b) A seismic stations network used as a TRM and the corresponding tesselation of the Earth surface used to correct the uneven distribution.

reversed signal critical: on the one hand, it is necessary to have the longest signal possible in order to preserve and take advantage of the complexity of the wavefield as explained above; on the other hand, the difference in lateral heterogeneities between the real Earth and the model might have an increasing influence with increasing time. However, at very long periods (larger than 200s), the influence of lateral heterogeneities is small and therefore not critical: the PREM model [*Dziewonski and Anderson*, 1981] is a very good approximation of the real Earth and accurate enough to provide a good agreement between observed and synthetic seismograms at very long periods. For this reason and because of computational cost, we chose to limit the following experiments to long periods for a first step.

[5] In global seismology, a time reversal experiment will consist in transforming the global network of seismic stations into an "active array". A station is a receiver and a recorder of the displacement field ($\mathbf{u}(\mathbf{x}, t)$), but also becomes an emitter of time-reversed waves which are numerically propagated. The displacement is sent back as an excitation force $\mathbf{f}_i(\mathbf{x}, t) = \sum_{r=1}^{N} A_r \mathbf{u}_i(\mathbf{x}_r, T - t)\delta(\mathbf{x} - \mathbf{x}_r)$, where $\{\mathbf{x}_r\}$ is the position set of stations. The coefficient A_r allows a station weighting.

[6] To begin, a series of purely synthetic experiments was performed in the long period range (T ≥ 150s). By synthetic numerical test, we mean that both the forward and backward propagation are numerically performed. The whole description of these tests as well as the corresponding figures and movies are found at the following address: http://www.gps.caltech.edu/~carene (mirror website at http://www.ipgp.jussieu.fr/~larmat). These tests showed that we obtain a good focusing at the right place and the right time by backpropagating only the vertical component of seismograms, provided that a large enough number of receivers (more than 100) is used, and is ensuring an azimuthal coverage around the seismic source as uniform as possible. In order to compensate for the uneven spatial distribution of stations, the amplitude of seismograms is decreased or increased through the coefficient A_r. This latter is computed according to the surface of the Voronoi cells which quantify the degree of isolation of a station (see Figure 1). The fact that using only the vertical component is sufficient for a good focusing means that this component contains enough

phase information to construct by interferences the correct backward Rayleigh waves which here dominate the wavefield given the frequency range. All further experiments are thus performed with a null horizontal excitation. An optimum value for the time duration is 8000s, which enables us to time reverse the first 2 wavetrains traveling in opposite directions. We then performed TR experiments with the data of the Peru event (23 June 2001) in 1D-model PREM [*Dziewonski and Anderson*, 1981] and a 3D tomographic model (SAW12D [*Li and Romanowicz*, 1996]). In fact, the improvement associated with 3D-model, is not, at this stage, very significant, which can be explained, by the small amplitude of lateral heterogeneities at very long periods (T > 200s). So, a good compromise for these first experiments on real data consists of making time reversal propagation into 1D PREM. Finally, synthetic seismograms with a finite source in the Sumatra area show that the primary effect is to lengthen the focusing time. It can be observed, as expected, that the focusing starts at the point and time of the last ruptured point and ends up at the initial point and time of rupture. Therefore, the time reversal process can be very useful for investigating the spatio-temporal rupture history.

3. Time Reversal Experiments Applied to the Great Sumatra-Andaman Earthquake

[7] On December 26, 2004 the subduction zone starts to rupture in the Northern part of Sumatra up to the Andaman Islands, approximately 1200 km away. A special issue of Science [*Lay et al.*, 2005; *Ammon et al.*, 2005; *Park et al.*, 2005] was devoted to the first results obtained from the investigation of seismic and other geophysical data. This event lasted about 6–7 minutes and it is the largest earthquake to have occurred since the Chile earthquake in 1960 and the Alaska earthquake in 1964 and since the advent of the Broadband Digital Seismology Network [*Romanowicz and Giardini*, 2001].

[8] After the deconvolution of the instrument response and a pass-band frequency filtering, 165 stations amongst the different networks of the FDSN (Federation of Digital Seismograph Network) were selected for the good quality of
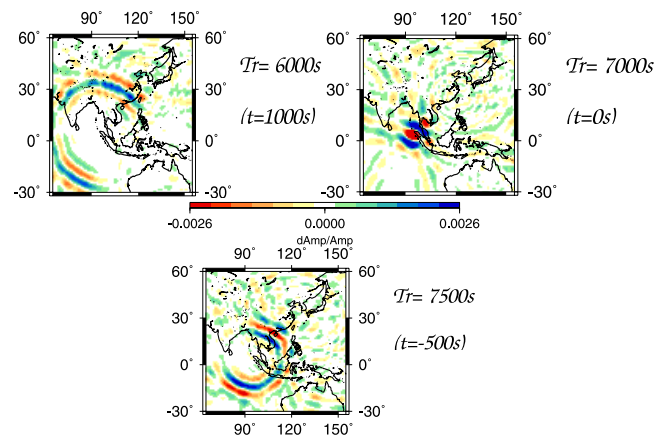

Figure 2. Vertical component of the time-reversed field at different times for the giant Sumatra-Andaman event. *t* is the absolute real time; Tr is the reversed time and Tr = 7000s corresponds to source initial time (t = 0s).
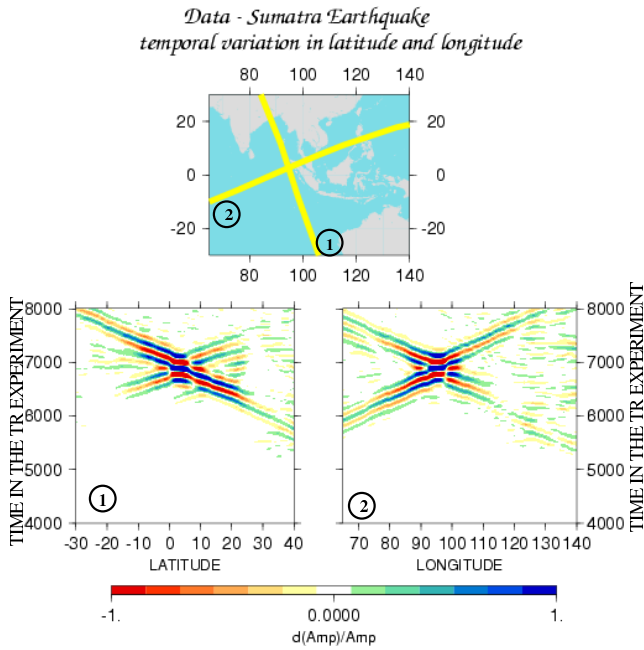
Figure 3. Application of time reversal method to data of Sumatra-Andaman earthquake (3.09°N, 94.2°6E); The time 7000s corresponds to the origin time. The 2 cross-sections along the yellow lines are displayed: on the left, a near latitudinal cross-section ($\sim$ along the fault plane) showing a strong asymmetry, on the right an orthogonal cross-section.

their vertical records. They ensure a good azimuthal coverage around the epicenter. We time-reverse a 8000s-long time-window (movie S^1). The origin of the earthquake corresponds to $t_0 = 1000s$, i.e., to a reversed time Tr of 7000s. Figure 2 shows three snapshots of the time-reversed wavefield at different times $Tr = 6000s$, 7000s and 7500s. The maximum focusing is observed at the time ($Tr = 7000 - 50$ s (± 20 s) and at the right spatial location: at latitude 3°N and longitude 95°E (± 200 km). The focal spot volume is relatively large due to the very long wavelength content of the seismograms and so limits the precision of the location. Our result is coherent with the estimated hypocenter that follows the initial time of about 120 s (Harvard CMT solution). It must be pointed out that we do not create an exact time-reversed replica of the earthquake. Indeed, the waves do not stop after focusing but continue to propagate displaying an almost circular wavefront. This is due to the fact that the source is not replaced by its time-reversed version, i.e., a sink which would absorb all the converging front [*de Rosny and Fink*, 2002].

[9] Two cross-sections of the displacement $\mathbf{u}(\theta, \phi, Tr)$ (where θ is the latitude, ϕ, the longitude) are extracted for two lines, parallel (basically latitudinal cross-section) and orthogonal to the plate boundary (longitudinal cross-section). They are shown in Figure 3 for reversed times from 4000s to 8000s. On both cross-sections, we see that when focusing occurs, seismic waves map the fault plane with a different sign in amplitude on either side of the fault. The focusing for the longitudinal cross-sections is more symmetrical before and after the focusing, whereas a very pronounced asymmetry in amplitude can be seen on the latitudinal cross-section as soon as $Tr = 6000s$ ($t = t_0 +$

1000s), suggesting a very strong directivity effect. It is not an artifact due to the uneven station distribution which is corrected (by A_r). Data inversion for a pre-shock on Nov. 2, 2002 does not show this asymmetry (auxiliary material Figure S1[1]). We have to bear in mind that the first observed point of refocusing in the TR experiment corresponds to the last part of the actual rupture and that, when waves start diverging, this point can be associated with the initial rupture point. Thus we observe on both cross-sections that the rupture starts approximately at 3°N, 98°E. The final latitude is difficult to determine due to the strong directivity of the source but seems to be located between 10°N and 20°N.

[10] In order to refine the source imaging even with this long period range, we made a quantitative comparison between the time-reversal experiments of the Great Sumatra earthquake of Dec 26, 2004 and a large pre-shock on Nov. 2, 2002 (lat 3.0°N, long. 96.2°E, depth 33 km, $M_S = 7.6$; $t_0 = 01:26:11$). For the finite source, the time-reversed field at the focalisation time is: $u_r^1 = S^1(\theta, \phi, t) \otimes \mathcal{TR}_{Net}^1(\theta, \phi, t)$, where S^1 is the real spatio-temporal history of the rupture and $\mathcal{TR}_{Net}^1$ the TR operator for a network of stations. For the point source of 2002, $u_r^2 = \mathcal{TR}_{Net}^2(\theta_0^2, \phi_0^2, t_0^2)$ as S^2 is a dirac function in space and time. As the stations are far away compared to the extent of the rupture, we can consider as a first though rough approximation that $\mathcal{TR}^1 \approx \mathcal{TR}^2$, so the TR imaging can be refined by deconvolving u^1 by u^2, both obtained with 121 common stations. The deconvolution is performed by a division of the space and time Fourier transforms. Figure 4 displays the space-time deconvolved cross-section along the fault plane. The zeros correspond to the latitude and origin time of the smaller event. The first maximum of energy is correctly centered at the location in time and space of the epicenter. We perfectly observe the migration from the south to the north. The energy is significantly above the noise level up to 260s for a rupture propagation of 900 km, providing a rupture velocity around 3.5 km/s. This spatio-temporal history might be improved in the future by considering shorter periods.

4. Discussion

[11] Our numerical experiments showed that the concept of time reversal can be successfully applied to real seismic data, and that, except a good velocity structure model, no *a priori* knowledge is necessary for locating the seismic source in both time and space. We can progressively follow, the spatial wavefield backpropagation and the reconstruction of the refocusing area. The maximum amplitude of time-reversed waves corresponds to the correct time and location, for the Sumatra-Andaman earthquake and a pre-shock in 2002. By comparing the two time-reversed wave field, we retrieve a rupture process coherent with other studies.

[12] So far, our time reversal method does not provide much more information regarding the seismic rupture than other studies [*Lay et al.*, 2005; *Ammon et al.*, 2005; *Park et al.*, 2005] or back-projection methods using a very dense array of short-period instruments [*Ishii et al.*, 2005], or array seismol-
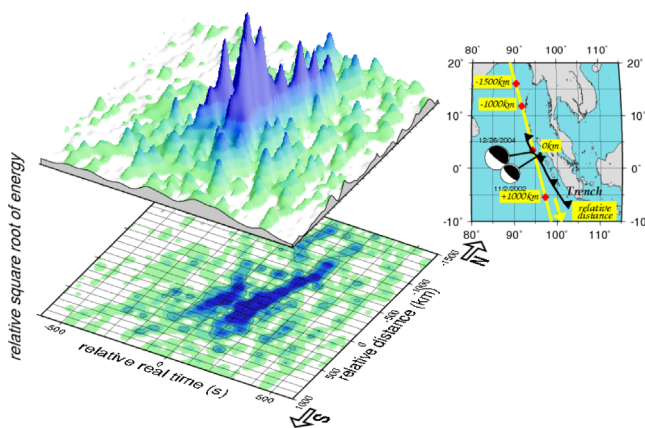

Figure 4. Approximate space-time rupture history in absolute time for the Great Sumatra-Andaman earthquake obtained by deconvolution from the pre-shock of Nov. 2, 2002 along the latitudinal cross-section of Figure 3 (yellow line). −1500 km (resp. 1000 km) is the North (resp. South) of the cross-section (yellow line).

ogy with broadband data [*Krüger and Ohrnberger*, 2005]. These latter methods only use the first arrivals of P-waves to gain insight with a high resolution in a limited area around the epicenter whereas we reconstruct everywhere the reverse movie of the whole wavefield but at long period so far. There is no theoretical problem to apply the TR technique to shorter periods using 3D heterogeneous anisotropic, anelastic global tomographic models. We can also imagine many other applications of the time reversal method. For example, it might be used for the automatic localization of earthquakes and nuclear explosions and for the investigation of unknown sources, causing seismic hum [*Suda et al.*, 1998; *Rhie and Romanowicz*, 2004], silent earthquakes [*Beroza and Jordan*, 1990] or glacial earthquakes [*Ekstrom et al.*, 2003]. Finally, we recall the strong connections between tomographic techniques and time-reversal field [*Tarantola*, 1988; *Tromp et al.*, 2005].

References

Ammon, C., et al. (2005), Rupture process of the 2004 Sumatra-Andaman earthquake, *Science*, *308*, 1133–1139.
Beroza, G., and T. Jordan (1990), Searching for slow and silent earthquakes, *J. Geophys. Res.*, *95*, 2485–2510.
Capdeville, Y., E. Chaljub, J.-P. Vilotte, and J.-P. Montagner (2003), Coupling spectral elements and modal solution: A new efficient tool for numerical wave propagation in laterally heterogeneous Earth models, *Geophys. J. Int.*, *152*, 34–67.
de Rosny, J., and M. Fink (2002), Overcoming the diffraction limit in wave physics using a time-reversal mirror and a novel acoustic sink, *Phys. Rev. Lett.*, *89*(12), 124,301.
Dziewonski, A., and D. Anderson (1981), Preliminary reference Earth model, *Phys. Earth Planet. Inter.*, *89*, 297–356.
Ekstrom, M., M. Nettles, and G. Abers (2003), Glacial earthquakes, *Science*, *302*, 622–624.
Fink, M. (1996), Time reversal in acoustics, *Contemp. Phys.*, *37*(2), 95–109.
Fink, M. (1997), Time reversed acoustics, *Phys. Today*, *50*(3), 34–40.
Fink, M., G. Montaldo, and M. Tanter (2003), Time reversal acoustics in biomedical engineering, *Annu. Rev. Biomed. Eng.*, *5*, 465–497.
Gilbert, F., and A. Dziewonski (1975), An application of normal mode theory to the retrieval of structural parameters and source mechanisms from seismic spectra, *Philos. Trans. R. Soc., Ser. A*, *278*, 187–269.
Ishii, M., P. Shearer, H. Houston, and J. Vidale (2005), Extent, duration and speed of the 2004 Sumatra-Andaman earthquake imaged by the Hi-Net array, *Nature*, *435*, 933–936.
Krüger, F., and M. Ohrnberger (2005), Spatio-temporal source characteristics of the 26 December 2004 Sumatra earthquake as imaged by teleseismic broadband arrays, *Geophys. Res. Lett.*, *32*, L24312, doi:10.1029/2005GL023939.
Lay, T., et al. (2005), The great Sumatra-Andaman earthquake of 26 December 2004, *Science*, *308*, 1127–1133.
Li, X. B., and B. Romanowicz (1996), Global mantle shear-velocity model developed using nonlinear asymptotic coupling theory, *J. Geophys. Res.*, *101*, 22,245–22,272.
Park, J., et al. (2005), Earth free oscillations excited by the 26 December 2004 Sumatra-Andaman earthquake, *Science*, *308*, 1139–1144.
Rhie, J., and B. Romanowicz (2004), Seismic hum, *Nature*, *431*, 552–555.
Rietbrock, A., and F. Scherbaum (1994), Acoustic imaging of earthquake sources from the Chalfant Valley, 1986, aftershock series, *Geophys. J. Int.*, *119*, 260–268.
Romanowicz, B., and D. Giardini (2001), The future of permanent seismic networks, *Science*, *293*, 2000–2001.
Suda, N., K. Nawa, and Y. Fukao (1998), Earth's background free oscillations, *Science*, *279*, 2089–2091.
Tarantola, A. (1988), Theoretical Background for the Inversion of Seismic Waveforms, Including Elasticity and Attenuation, *Pure Appl. Geophys.*, *128*(1–2), 365–399.
Tourin, A., A. Derode, and M. Fink (2001), Sensitivity to perturbations of a time-reversed acoustic wave in a multiple scattering medium, *Phys. Rev. Lett.*, *87*, 274–301.
Tromp, J., C. Tape, and Q. Liu (2005), Seismic tomography, adjoint methods, time reversal and banana-doughnut kernels, *Geophys. J. Int.*, *160*, 195–216.

————————————
Y. Capdeville, E. Clévédé, and J.-P. Montagner, Laboratoire de sismologie globale, Institut de Physique du Globe de Paris, 4 Place Jussieu, Paris F-75252, France. (capdevil@ipgp.jussieu.fr; clevede@ipgp.jussieu.fr; jpm@ipgp.jussieu.fr)
M. Fink and A. Tourin, Laboratoire Ondes et Acoustique, ESPCI, 10 rue Vauquelin, F-75231 Paris, France. (mathias.fink@espci.fr; arnaud.tourin@espci.fr)
C. Larmat, Seismological Laboratory, California Institute of Technology, 1200 East California Boulevard, MS 252-21, South Mudd Building, Room 266, Pasadena, CA 91125, USA. (carene@gps.caltech.edu)